# Applications of Digital Twin for Autonomous Zero-Touch Optical Networking [Invited]

Luis Velasco*, Mariano Devigili, and Marc Ruiz
*Optical Communications Group - Universitat Politècnica de Catalunya.* Barcelona, Spain
*luis.velasco@upc.edu

***Abstract*—Huge efforts have been paid lastly to study the application of Machine Learning techniques to optical transport networks. Applications include Quality of Transmission (QoT) estimation, failure and anomaly detection, and network automation, just to mention a few. In this regard, the development of Optical Layer Digital Twins able to accurately model the optical layer, reproduce scenarios, and generate expected signals are of paramount importance. In this paper, we introduce two applications of Optical Layer Digital Twins namely, misconfiguration detection and QoT estimation. Illustrative results show the accuracy and usefulness of the proposed applications.**

***Keywords—Optical Digital Twin, Network Automation***

## I. Introduction

Digital twins have been proposed as a key tool for network automation, as they can provide a holistic representation of the network with high accuracy and, simultaneously, low computational complexity [1]. A digital twin should generate, among others, expected signals that can be compared with those obtained from the network. In that way, deviations between the observed and the expected signals can be detected and used for, e.g., soft-failure and anomaly detection [2], [3]. Several tools can be used to develop digital twins for optical communications, including the open-source project GNPy [4] that implements the Gaussian Noise (GN) model [5] to estimate signal's Linear Interference (LI) noise and Non-Linear Interference (NLI) noise powers and thus, the Quality of Transmission (QoT) of optical signals. Based on GNPy, some works in the literature have proposed failure management solutions [6]. In parallel, Machine Learning (ML) has shown its potential application for network automation [7]. The low computational requirements of ML models for inference, once trained, make ML very attractive to solve hard computational problems.

In our previous paper in [8], we proposed an optical time domain digital twin named OCATA based on Deep Neural Networks (DNN) to model how LI and NLI noise from network components (i.e., reconfigurable optical add/drop multiplexers (ROADMs) and optical links) impact in-phase and quadrature (IQ) optical constellations. OCATA can be used to discover network configuration; specifically, we explored its potential to find the most likely configuration of transparent intermediate network segments in mixed disaggregated-proprietary scenarios. OCATA has been applied also for degradation detection [9].

978-3-903176-54-6 © 2023 IFIP

In this paper, we explore two new applications of OCATA: *i*) lightpath length misconfiguration detection; and *ii*) QoT estimation.

## II. OCATA Optical Digital Twin

Discrete optical IQ constellation samples $X$ are defined by a sequence of symbols $x \in X$, each of them represented by a complex number where the real and imaginary parts are the I and Q components of the optical signal, respectively. Such sequence can be represented as an IQ optical constellation, where every symbol belongs to one among $m$ constellation points.

Fig. 1 presents two input samples $X$ from a $m$=16 quadrature amplitude modulated (QAM) optical signal when they are received after 400 km (Fig. 1a) and after 1200 km (Fig. 1b). We apply Gaussian Mixture Models (GMM) [10] to characterize a given optical constellation sample as a set of bivariate Gaussian distributions with one distribution per constellation point. For illustrative purposes, Fig. 1 includes the GMM fitting of the two optical constellation samples $X$.

Then, for every input sample $X$, a set of semi-supervised constellation features $Y$ that summarizes $X$ is generated. We denote $Y^i$ the vector of features characterizing the constellation point $i$. In particular, GMM fitting is used to characterize every constellation point $i$ by means of 5 features representing the real and imaginary mean position in the constellation ($\mu$) and the real and imaginary variance and symmetric covariance terms ($\sigma$) that the symbols belonging to the constellation point $i$ experience around the mean, i.e., $Y^i=[\mu^I,\mu^Q,\sigma^I,\sigma^Q,\sigma^{IQ}]^i$. Note that the higher the LI and NLI impairments affecting the optical

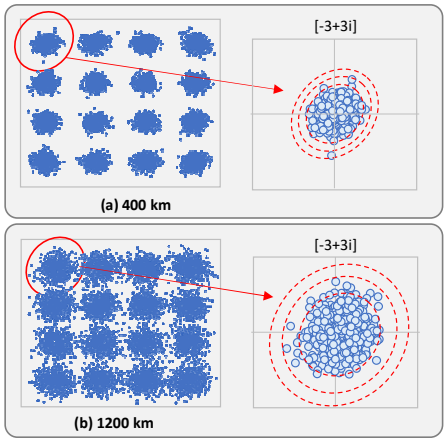


Fig. 1. GMM fitting for optical IQ constellation features extraction

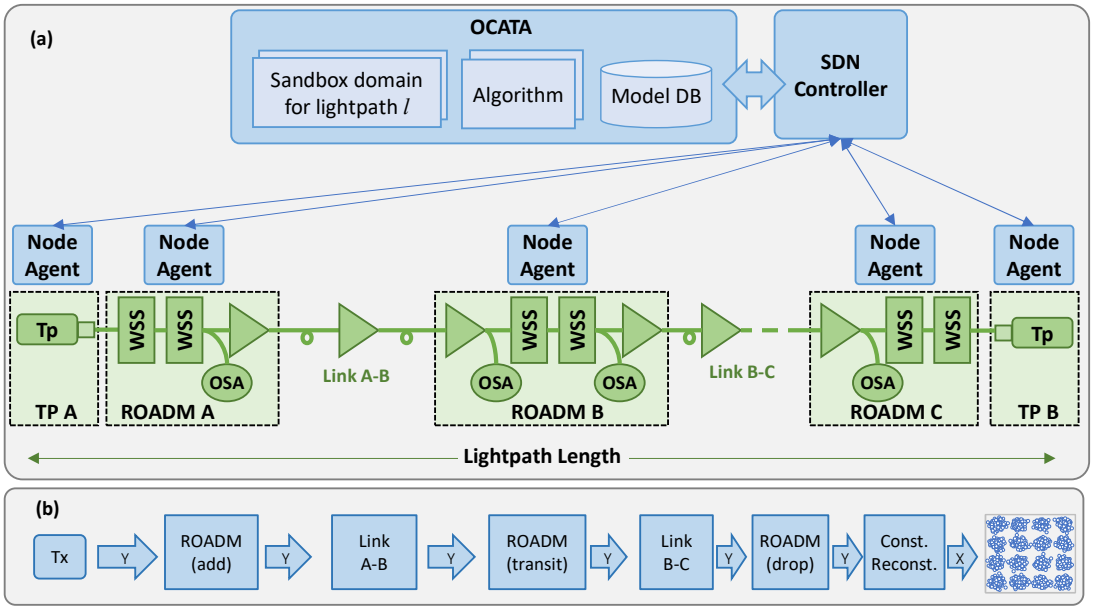


Fig. 2. Architecture and lightpath example (a) and OCATA modeling (b).

signal, the more dispersed the symbols are, which makes constellation characterization more challenging.

Fig. 2 represents a lightpath in the optical data plane (a) and its OCATA digital twin (b). We assume that every optical node is controlled by a local node agent that configures the underlying optical devices and collates telemetry data from them. On top of the architecture, a software-defined networking (SDN) controller connects to the node agents and to a layer modeling the data plane that includes OCATA components: *i*) a model DB with DNN models for the different network components. Different component models are pre-trained for components with different characteristics, like fiber length and type, and number of spans in the case of optical links. Component models propagate input features after being impacted by the impairments of the specific network component being modeled, and produce output features. Such component models can be concatenated to represent end-to-end lightpaths, so the output features from one component model become the input of the next one. Then, creating a digital twin for a lightpath consists in concatenating models for the specific elements in the route of the lightpath; *ii*) a sandbox domain, that is used to compose the models for the end-to-end lightpaths; and *iii*) a set of algorithms that analyze the features of the signals received and compare to those generated by the models.

As an example, Fig. 2 represents a lightpath in the optical data plane and its OCATA digital twin. To reduce complexity, only the features of a few selected constellation points are propagated. Then, a constellation reconstruction module generates the features of the non-propagated constellation points based on the received features to complete the IQ optical constellation.

## III. Applications

In this section, we extend the basic functionalities of OCATA by: *i*) training specific DNNs that use basic and/or new features for specific use cases, like QoT and lightpath length estimation; *ii*) adding new features to vector $Y$, so as to improve the representation of sample $X$; and *iii*) proposing new algorithms for lightpath length misconfiguration detection.

Algorithm 1. Misconfiguration Detection

**INPUT**: $Y, f, g$
**OUTPUT:** $\langle misconf, dRx \rangle$

```
misconf ←False
for each y in Y do
    <l_y, h_y>←getRange(f, y)
    if y not in [l_y, h_y] then
        misconf ←True
        break
return <misconf, g(F)>
```

### A. Lightpath length misconfiguration detection

In this first use case, two DNN models are trained for the characteristics of the lightpath (i.e., length, modulation format, symbol rate, etc.). Specifically, model $f$ is used for lightpath length misconfiguration detection, whereas model $g$ estimates real lightpath length.

Algorithm 1 presents the main procedure, which receives features $Y$ from an optical constellation sample, as well as the two trained models. Misconfiguration detection is carried out using model $f$, which specifies the range $[l_y, h_y]$ that each of the features $y \in Y$ should be in case of the received signal has propagated along the estimated lightpath length. Then, the algorithm checks every individual feature and only in the case that all are within the modeled range, we consider that the lightpath is properly configured. On the contrary, if the length of the lightpath is very different to the expected one, the distribution of the features would be different as well and found out of its modeled range. Finally, the result of the detection is returned jointly with the estimation of the distance provided by model $g$. This model was designed as a DNN with one input

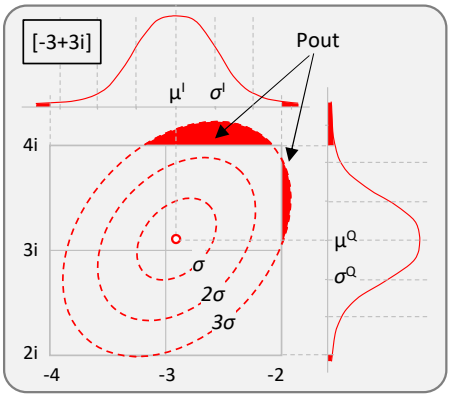


Fig. 3. Example of *Pout* feature for constellation point [-3,3*i*]

neuron per each feature, a number of hidden neurons in a single layer, and one single neuron for the output that estimates the distance (in km) where the Tx originating the received signal is likely to be.

### B. *QoT estimation*

We tackle the estimation of lightpaths' QoT, specifically the Bit Error Rate (BER), as a function of constellation features. Two different use cases can take advantage from such prediction: *i*) lightpath provisioning, where BER estimation can be used to validate that the expected QoT meets the required one. To this end, OCATA can be used to generate the expected signal and, from there, the expected BER is estimated; and *ii*) BER estimation during lightpath operation for QoT monitoring purposes, where collected optical constellations need to be analyzed. For both use cases, a DNN model is needed to estimate BER values in a meaningful range, e.g., from $10^{-5}$ to $10^{-2}$.

To this purpose, the basic features $Y$ defined in Section II can be used as inputs of a DNN model that estimates the BER. Note that $Y$ characterize the dispersion of symbols by means of bivariate Gaussian distributions and, in turn, such dispersion is related with BER.

Nevertheless, the characterization of the dispersion that $Y$ provides and its relation with BER is not trivial. In view of that, we propose adding a new feature, denoted as $Pout^i$, that computes the probability that a symbol initially transmitted in constellation point $i$ is detected in the Rx out of the detection area of such constellation point, denoted as $A^i$. $Pout^i$ is computed under the assumption that dispersion of symbols around constellation point $i$ follow the bi-variate Gaussian distribution characterized by $Y^i$. It is worth noting that this feature is more clearly related with the errors in the Rx.

Fig. 3 shows and example of $Pout^i$ feature for constellation point [-3+3i]. The contours represent the different levels of the bi-variate Gaussian distribution that characterize this constellation point for a given lightpath. For the sake of clarity, we depicted $\sigma$, $2\sigma$, and $3\sigma$ levels only; univariate marginal distributions are provided for both $I$ and $Q$ axes. The area highlighted in red in both bi-variate and marginal distributions represent the region that falls out of $A^i$, i.e., the square delimited by vertices (-4+4*i*) and (-2+2*i*). Hence, $Pout^i$ is formally defined as follows:

$$Pout^i = 1 - P(x \subset A^i | x \sim N(Y^i)) \quad (1)$$

Armed with this new feature, a DNN can be trained that take *Pout* as input and produce QoT estimation as output.

## IV. Results

For numerical evaluation purposes, a MATLAB-based digital coherent system was implemented. We assume a 11-channel WDM scenario, where all channels are configured with the same modulation format and symbol rate (i.e., dual polarization 16QAM @64 GBd), and 75 GHz channel spacing. At the Tx side, pseudo-random binary sequences of $2^{20}$ bits are modulated to create $2^{18}$ symbols and shaped by a root-raised cosine filter with a 0.06 roll-off factor. An ideal optical multiplexer aggregates individual signals with optical channel power of -1 dBm and creates the WDM channel to be propagated through the optical line system consisting of a number of 80 km of standard single mode fiber (SSMF) spans characterized by attenuation factor of 0.21 dB/km, dispersion parameter of 16.8 ps/nm/km, and nonlinear parameter of 1.14 $(W \cdot km)^{-1}$. An erbium doped fiber amplifier with noise figure of 4.5 dB ideally compensates each span losses. The pulse propagation along the SSMF is modelled by solving the nonlinear Schrödinger equation using the split-step Fourier method [11] with propagation step size of 100 m. Finally, DSP blocks capable to perform an ideal dispersion compensation and phase recovery are considered in the Rx.

### A. *Lightpath length misconfiguration detection*

For this application, we generated a large dataset comprising of 4,000 signal samples, with 2048 symbols each, for the lightpath under analysis with lengths ranging from 80 km to 2,000 km, i.e., from 1 to 25 spans. Data were split for: *i*) training and testing application's models; and *ii*) validating the overall procedure.

Let us first demonstrate the potential usefulness of the features. Fig. 4a shows the difference of the computed mean values from the expected constellation point centroid ($\Delta\mu$) for constellation point (-3+3i) as a function of the lightpath length, where each point averages the results of 10 samples. We observe that the constellation point's center moves away from the expected center when the lightpath length increases. The correlation between features and lightpath length is even stronger in terms of variance components. Fig. 4b shows a clear increase of the variance from short to longer paths. Therefore, we can conclude that the proposed features summarize useful information about lightpath length, which is a necessary condition for highly accurate models.

Next, we study the performance of the misconfiguration detection model. To this aim, we trained one model $f$ for each of the considered path lengths and evaluated each model with enough testing samples to guarantee that no false misconfiguration detection is produced when a sample of the same distance is processed. Then, for each length, we run the detection procedure in Algorithm 1 with samples of shorter distance than that of the actual one. Detection accuracy reduces

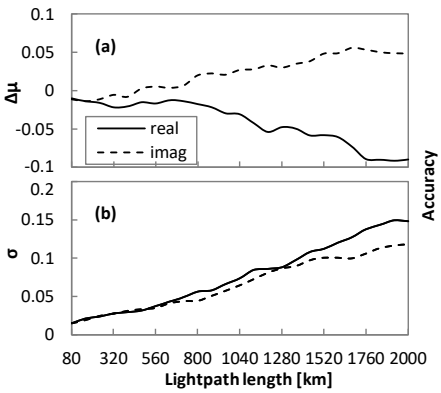


Fig. 4. Mean deviation (a) and variance (b) vs lightpath length

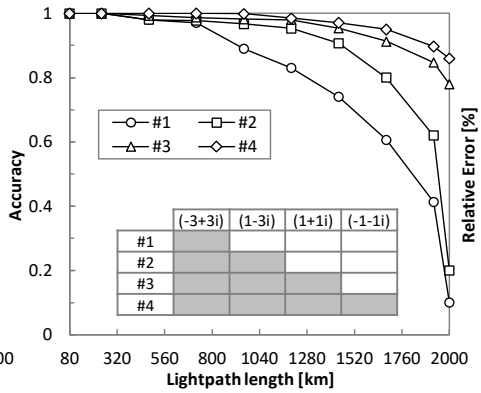


Fig. 5. Accuracy of misconfiguration detection vs lightpath length

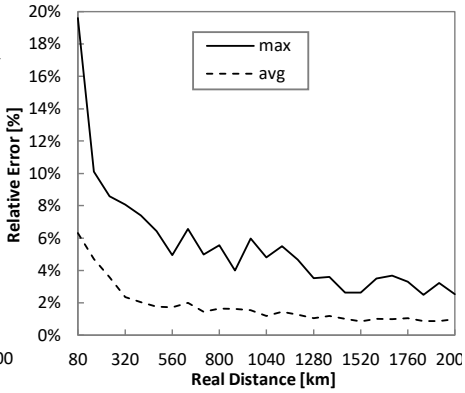


Fig. 6. Max and avg relative error in distance prediction

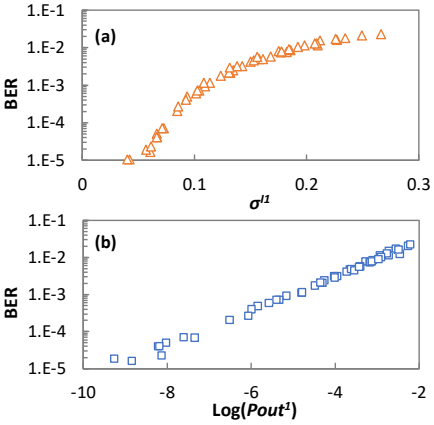


Fig. 7. Correlation of BER with variance and *Pout* features

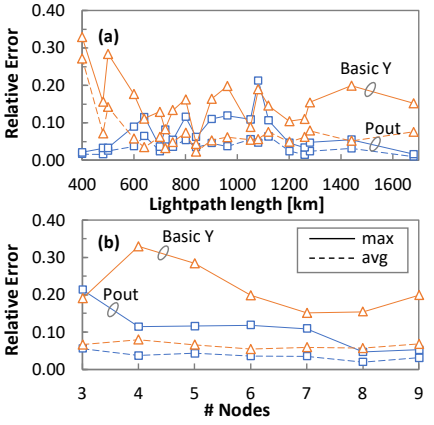


Fig. 8. Max and avg relative error of DNNs vs length and number of nodes

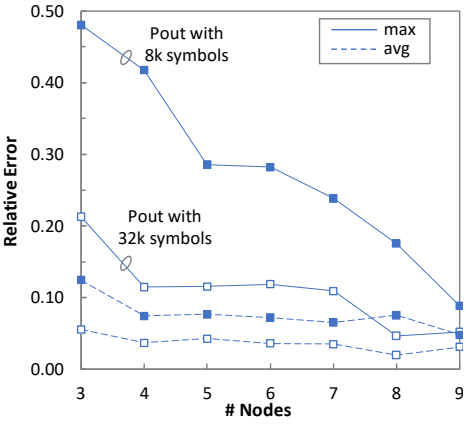


Fig. 9. Influence of constellation size on the relative error.

with the real distance of the lightpath; Fig. 5 shows the detection accuracy of each model for samples with only one span less than the length of the lightpath. We reproduced the analysis for several subsets of constellation points (the inset table in Fig. 5 specifies the points selected in each case). From the results, we conclude that the selected 4 constellation points covering different parts of the constellation achieves 100% of misconfiguration detection accuracy for paths up to 1,000 km, and such accuracy decreases down to 90% for paths of 2,000 km.

Finally, let us now focus on the distance estimation accuracy. Model $g$ was implemented as a DNN with the following configuration: *i*) features $Y$ from the 4 selected constellation points as inputs; *ii*) 2 hidden layers with 12 and 6 neurons, respectively, using the hyperbolic tangent (*tanh*) as activation function; *iii*) the estimated lightpath length as output neuron; *iv*) root mean squared propagation as optimization algorithm; *v*) training stage with up to 5,000 epochs; and *vi*) mean square error as loss function.

Fig. 6 shows the average and maximum relative estimation error of the model. We observe that the accuracy of the model heavily depends on the real distance; short distances might include larger error than longer ones.

## B. *QoT estimation*

For this use case, we studied 12 different scenarios of lightpaths with 2, 3, 7, and 9 hops, and 2, 3, 6, and 7 fiber spans, and 50, 60, 80 km. At each network node, the optical constellations were collected and employed to evaluate the BER of the received optical signal. As on the previous application, data were split for: *i*) training and testing application's models; and *ii*) validating the overall procedure.

Two different low complexity DNNs have been considered, with: *i*) lightpath length in km, number of nodes, and considered features from 4 selected constellation points as inputs; *ii*) 2 hidden layers with 10 neurons, using tanh as activation function; *iii*) the log10 of the BER as output neuron; *iv*) root mean squared propagation as optimization algorithm; *v*) training stage with up to 5,000 epochs; and *vi*) mean square error as loss function. The first DNN, named *basic Y*, considered basic features $Y^i=[\mu^I,\mu^Q,\sigma^I,\sigma^Q,\sigma^{IQ}]^i$, whereas the second DNN considered $Pout^i$. Then, the former DNN has 22 input neurons, whereas the latter one only 6.

For illustrative purposes, Fig. 7a, b shows the correlation between BER and $\sigma^I$ and $Pout^I$ features, respectively, computed from constellation point (-3+3*i*). We observe a linear

correlation of BER and $Pout^l$ in logarithmic scale, being that with $\sigma^l$ nonlinear. This result anticipates better accuracy of the *Pout* DNN model, as we observe in Fig. 8, where both models are compared as a function of lightpath length and number of nodes in terms of maximum and average relative error. Although in both cases the error is more than acceptable, the *Pout* DNN model provides noticeable accuracy.

Finally, Fig. 9 studies the relationship between the accuracy of the *Pout* DNN and the number of symbols in the collected constellations that are used for training and as input for estimation. Note that the larger the number of symbols, the higher the accuracy and robustness of the GMM fitting. To this end, collected constellations with $|X|=2^{18}$ symbols were randomly down-sampled to $2^{13}$ (labeled *8k*) and $2^{15}$ (labeled *32k*) symbols. We observe how DNN accuracy reduces remarkably when the number of symbols collected decreases.

## V. CONCLUSIONS

Two new applications of a digital twin for the optical layer, named OCATA, have been proposed and evaluated through simulation. In OCATA, every optical constellation point is modelled as a bi-variate Gaussian distribution characterized by its I and Q means and variances and the covariance, which are called *basic features*. OCATA includes: *i*) DNN models that propagate features of a network components based on the impact of LI and NLI noise. Those models can be concatenated to model end-to-end lightpaths; and *ii*) algorithms and DNN models that use features from optical constellations generated by OCATA or collected from the network. Extensions to both, the considered features that characterize optical constellations, as well as algorithms and DNN models have been proposed for lightpath length misconfiguration detection and BER estimation.

For the misconfiguration detection, it was shown that when real distances are short, detection achieves high accuracy, which decreases for long distances. A distance estimation application was also proposed, which exhibited opposite behaviors as the misconfiguration detection, i.e., it achieved high accuracy for long distances and decreased for short distances. Therefore, a combined analysis of both detection and prediction achieves remarkable accuracy.

As for BER estimation, two possible applications where highlighted, for lightpath provisioning purposes, where the input constellation comes from OCATA and for monitoring purposes, where the input constellation has been collected from the network. A new feature, named *Pout*, was proposed accounting for the probability of a symbol to be out of the area reserved for the intended constellation point. DNNs were trained considered *Pout* as input only and another considering the basic features. A linear correlation between *Pout* and BER was observed, which translated on a very accurate DNN for BER estimation. Finally, the impact of the size of the constellation on DNN accuracy was shown, where size with 32k symbols provide good estimation accuracy.

## ACKNOWLEDGEMENT

The research leading to these results has received funding from the European Community through the MSCA MENTOR (G.A. 956713) and the HORIZON SNS JU SEASON (G.A. 101096120) projects, the AEI through the IBON (PID2020-114135RB-I00) project, and by the ICREA institution.

[1] D. Wang, Z. Zhang, M. Zhang, M. Fu, J. Li, S. Cai, C. Zhang, and X. Chen, "The Role of Digital Twin in Optical Communication: Fault Managements, Hardware Configuration, and Transmission Simulation," IEEE Communications Magazine, vol. 59, pp. 133-139, 2021.

[2] B. Shariati, M. Ruiz, J. Comellas, and L. Velasco, "Learning from the Optical Spectrum: Failure Detection and Identification [Invited]," IEEE/OPTICA Journal of Lightwave Technology, vol. 37, pp. 433-440, 2019.

[3] A. P. Vela, B. Shariati, M. Ruiz, F. Cugini, A. Castro, H. Lu, R. Proietti, J. Comellas, P. Castoldi, S. J. B. Yoo, and L. Velasco, "Soft Failure Localization during Commissioning Testing and Lightpath Operation [Invited]," IEEE/OSA Journal of Optical Communications and Networking, vol. 10, pp. A27-A36, 2018.

[4] V. Curri, "GNPy model of the physical layer for open and disaggregated optical networking [Invited]," IEEE/OPTICA Journal of Optical Communications and Networking, vol. 14, pp. C92-C104, 2022.

[5] P. Poggiolini, G. Bosco, A. Carena, V. Curri, Y. Jiang, and F. Forghieri "The GN-Model of Fiber Non-Linear Propagation and its Applications," IEEE/OPTICA Journal of Lightwave Technology, vol. 32, pp. 694-721, 2014.

[6] S. Barzegar, M. Ruiz, A. Sgambelluri, F. Cugini, A. Napoli, and L. Velasco, "Soft-Failure Detection, Localization, Identification, and Severity Prediction by Estimating QoT Model Input Parameters," IEEE Transactions on Network and Service Management (TNSM), vol. 18, pp. 2627-2640, 2021.

[7] D. Rafique and L. Velasco, "Machine Learning for Optical Network Automation: Overview, Architecture and Applications," IEEE/OSA Journal of Optical Communications and Networking, vol. 10, pp. D126-D143, 2018.

[8] M. Ruiz, D. Sequeira, and L. Velasco, "Deep Learning -based Real-Time Analysis of Lightpath Optical Constellations [Invited]," IEEE/OPTICA Journal of Optical Communications and Networking, vol. 14, pp. C70-C81, 2022.

[9] M. Devigili, M. Ruiz, S. Barzegar, N. Costa, A. Napoli, J. Pedro, and L. Velasco, "Degradation Detection and Severity Estimation by Exploiting an Optical Time and Frequency Digital Twin," in Proc. OPTICA Optical Fiber Communication Conference, 2023.

[10] N. Bouguila and W. Fao, *Mixture Models and Applications*, Springer, 2020.

[11] J. Shao, X. Liang, and S. Kumar "Comparison of Split-Step Fourier Schemes for Simulating Fiber Optic Communication Systems," IEEE Photonics Journal, vol. 6, pp. 1-15, 2014.